NATIONAL AERONAUTICS AND SPACE ADMINISTRATION

Technical Report 32-1452

Mariner Mars 1969 Sun Sensor Development

L. F. Schmidt

JET PROPULSION LABORATORY
CALIFORNIA INSTITUTE OF TECHNOLOGY
PASADENA, CALIFORNIA

January 1, 1970

NATIONAL AERONAUTICS AND SPACE ADMINISTRATION

Technical Report 32-1452

Mariner Mars 1969 Sun Sensor Development

L. F. Schmidt

JET PROPULSION LABORATORY
CALIFORNIA INSTITUTE OF TECHNOLOGY
PASADENA, CALIFORNIA

January 1, 1970

Prepared Under Contract No. NAS 7-100
National Aeronautics and Space Administration

Preface

The work described in this report was performed by the Guidance and Control Division of the Jet Propulsion Laboratory.

Contents

Figures

Abstract

The sun sensors are electro-optical devices used in the *Mariner* Mars 1969 attitude control system. These sensors provide two-axis error signals for turning the spacecraft toward the sun, such that the solar panels are illuminated. The sun sensors also provide continuous error signals for holding this position throughout the mission. A special sensor, the sun gate, provides an indication of whether the spacecraft is aligned to the sun within 4.5 degrees of true position in both axes. The operation of the sensors is described as well as the design, testing, and problems encountered.

Mariner Mars 1969 Sun Sensor Development

I. Introduction

In the *Ranger* and *Mariner* spacecraft, the sun is used as a celestial reference for pitch- and yaw-axis attitude control. The operating principle of the sun sensors in each of these spacecraft is basically the same, but the configuration and output characteristics of the sun sensor systems change from mission to mission, depending on the associated field of view and dynamic constraints. A *Ranger* flight set of sensors consists of the acquisition sensor assemblies and the cruise sensor assemblies. A *Mariner* flight set of sensors consists of the acquisition sensor assemblies, the cruise sensor assemblies, and the sun gate assembly. For the *Mariner* Mars 1969 program, a redesigned photodetector was used.

This report covers the design, fabrication, and testing of the sun sensors required to support the *Mariner* Mars 1969 mission. A flight set for this mission includes four acquisition sensor assemblies, two cruise sensor assemblies, and one sun gate assembly. The maximum total power required is 0.3 W. This power level, which is dissipated in the detectors, is dependent on the solar intensity and decreases to approximately 0.2 W at Mars encounter. The weight of the sun sensor set is 0.8 lb. It is presumed that the pointing accuracy of the sensors was well within the ± 1.4 mrad tolerance.

II. Theory of Operation

A. Operation of Acquisition and Cruise Sun Sensors

The operation of the acquisition and cruise sensors can be visualized by reference to Figs. 1 and 2 and the following description. Figure 1 illustrates the mechanical arrangement of the photodetectors; Fig. 2 is an electrical diagram for the detectors. The photodetectors contain cadmium sulfide as the light-sensitive material. Each detector is essentially a light-sensitive resistor that has a fully lit resistance of approximately 800 Ω at earth (1 solar constant), which increases to approximately 1215 Ω at Mars (0.433 solar constant).

The method of operation of a single-axis sensor system is as follows. In the sun-acquired position, the sunlit area of cruise detectors A and B is equal, as shown in Fig. 1, and the resistance of each detector is equal, which results in a null output voltage. When the spacecraft rotates slightly from the position shown, the sunlit areas of detectors A and B become unequal and produce unequal resistances. This condition in turn causes an unequal voltage drop across each of the detectors A and B, which results in an output signal. A clockwise rotation produces a negative output signal and a counterclockwise rotation produces a positive output signal. For large angles of

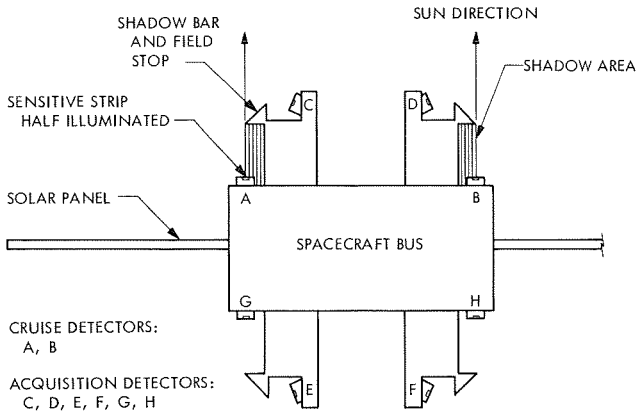

Fig. 1. Detector mechanical arrangement (single axis)

rotation, the acquisition detectors C, D, E, F, G, and H (Fig. 1) must be considered, since they are electrically energized by relay R1 (Fig. 2) at error angles of approximately 5 deg or greater. For clockwise error angles between approximately 5 and 89 deg, detectors A and C are both sunlit. Under this condition a negative output signal will result, since both detectors have a negative excitation voltage, and their paralleled resistance is less than the paralleled resistance of detectors B, D, F, and H, which are not sunlit. At any error angle, two or more detectors are sunlit, and the single-axis system depicted in Figs. 1 and 2 generates an output signal curve as shown in Fig. 3. Another axis, the same as depicted in Fig. 1, but oriented 90 deg about the spacecraft sun line, is required to produce pitch- and yaw-axis output signals. The complete system provides a 4π steradian field of view, which allows sun acquisition from any spacecraft position.

B. Operation of Sun Gate

In the operation of the sun gate, the structure provides a light-tight enclosure for each of two detectors of the same type used in the cruise and acquisition sensors. Each detector enclosure has a 0.070-in. diameter aperture. This aperture is accurately adjusted to allow solar energy to enter the enclosure and activate the detector whenever the spacecraft roll axis is aligned to within 8 deg of the spacecraft sun line. The minimum resistance occurs at a 0-deg error angle, as shown by the output resistance curve in Fig. 4. At minimum resistance the active area of the detector is completely illuminated by sunlight admitted by the aperture. The output resistance of the sun gate is

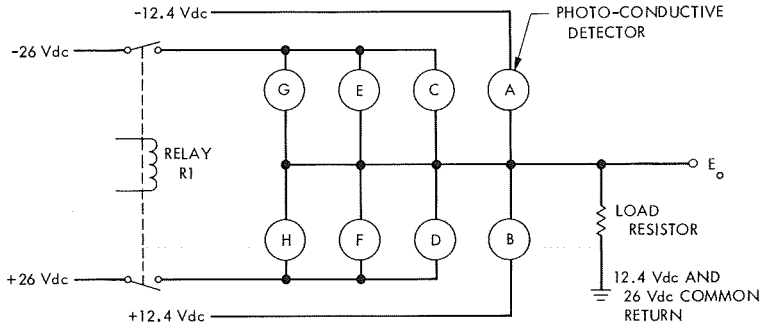

Fig. 2. Detector electrical diagram (single axis)

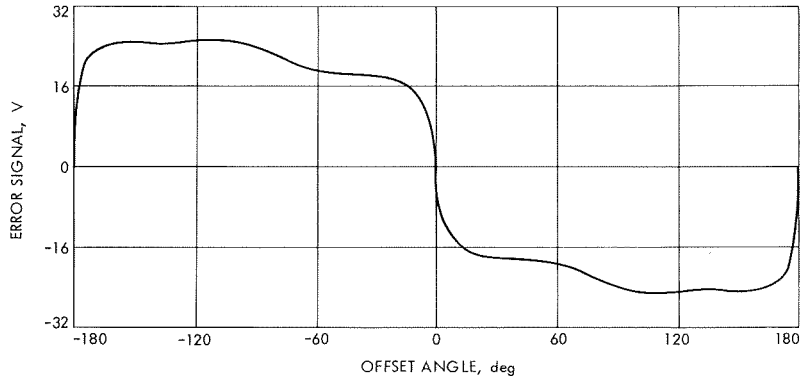

Fig. 3. Sun sensor system output curve

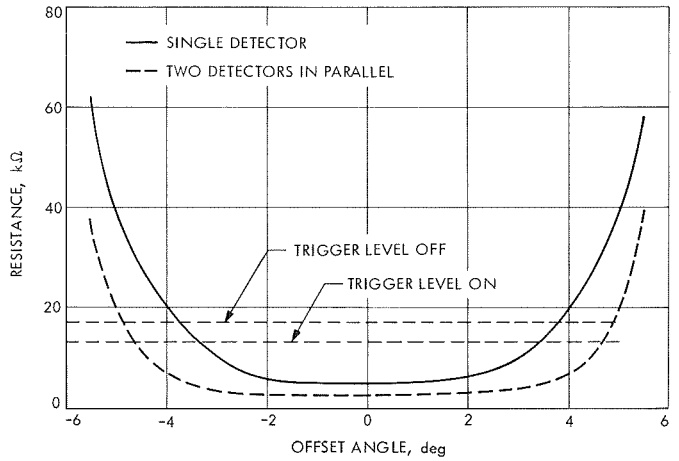

Fig. 4. Sun gate resistance curves

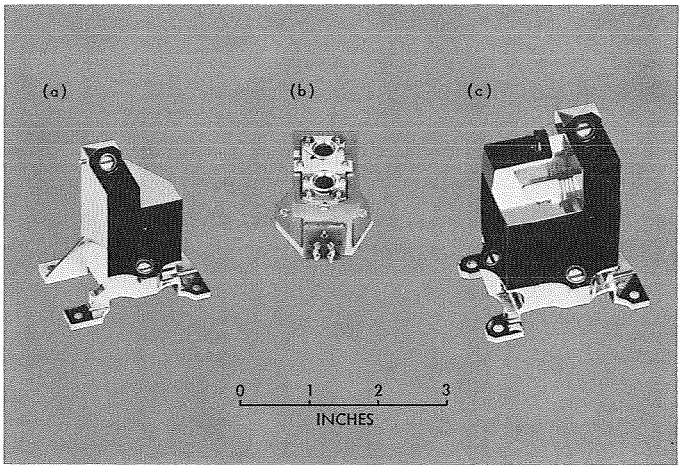

Fig. 5. Sun sensor flight set: (a) acquisition sensor, (b) sun gate, (c) cruise sensor

monitored by the attitude-control logic circuitry. This circuitry indicates sun acquisition whenever the resistance is below a predetermined value of approximately 13 kΩ. One of the events caused by a sun-acquisition signal is the de-energizing of the acquisition sun detectors through relay R1 shown in Fig. 2.

Two detectors wired in parallel are provided to increase the reliability of the sun gate. An open-circuit failure of either detector will change the level of the resistance curve, as shown in Fig. 4. This will alter the angle at which sun acquisition is indicated, but proper operation will continue. A shorted detector is many times more unlikely than an open circuit, since each detector has an electrode separation of 0.050 in. and is hermetically sealed to prevent foreign material from shorting across this gap.

III. Design and Fabrication

A. Design and Fabrication of Sun Sensors

The design of the *Mariner* Mars 1969 sun sensors was essentially the same as the *Mariner* Mars 1964 design, except that a modification was made to incorporate a new photodetector, which is housed in a TO-5 size transistor case having a window to admit solar radiation.

The *Mariner* Mars 1969 sun sensor flight set required four acquisition sensor assemblies, compared to two for *Mariner* Mars 1964, because of more severe field-of-view constraints imposed by the size and configuration of the scan platform. The acquisition sensors (Fig. 5a), which contain two detectors each, are mounted in Bays I, III, V, and VII on the lower ring of the spacecraft octagon structure.

The cruise assembly includes two cruise sensors (Fig. 5c), which are mounted on pedestals extending upward from the bay-IV and bay-VIII positions of the spacecraft octagon structure. Each cruise sensor assembly contains two acquisition detectors as well as two cruise detectors. The cruise detectors are located nearest the base plane. The cruise detector excitation voltage was reduced from the 16 V used in *Mariner* Mars 1964 to 12.4 V. This was done to reduce the power dissipation and consequently to improve the reliability of the photodetectors.

Two design modifications were made as a result of the vibration-induced detector failures (see Section IV). First, a resilient mount for the detector was designed to reduce the high g levels imposed on the detector assembly by virtue of its damping qualities. Second, a design modification was made in the photodetector to increase its vibration resistance. The time required to develop the resilient mount was minimum, but it was not known whether the proposed design changes in the detector could be made in time to meet the fabrication schedules for the sun sensors. It was therefore decided to immediately incorporate the resilient mount into the flight sensor design, and to develop a ruggedized photodetector as a concurrent back-up effort. This development is covered in Section V of this report.

The configuration of the photodetector resilient-mount assembly is shown in Fig. 6. The isolation washers (parts 4 and 5) are made of silicon rubber having a Shore durometer hardness of 35. A small amount of compression (from 5 to 15%) was used to encourage a sliding motion between the isolation washers and the contacting metal parts under vibration conditions. This was done to allow

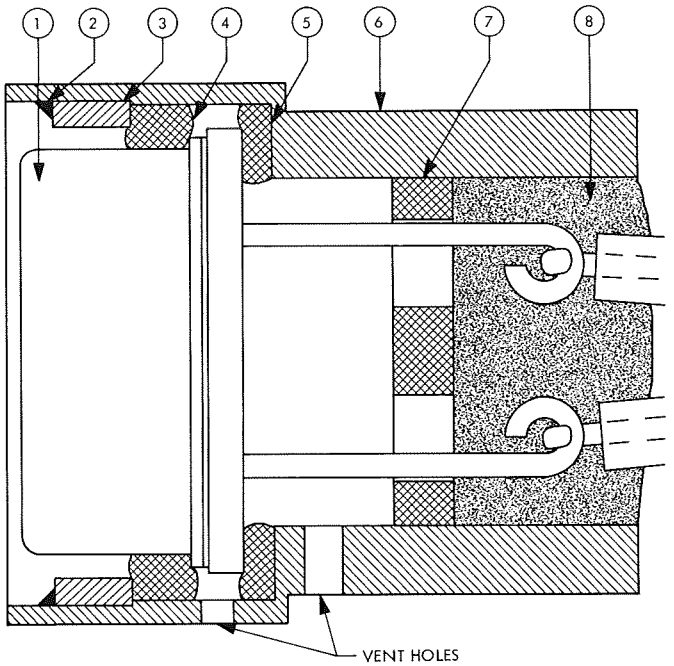

Fig. 6. Photodetector resilient-mount assembly

conversion of the kinetic energy to heat through the associated friction. This resilient-mount design was incorporated into the engineering prototype sun sensors for evaluation. The detectors used were rescreened at 70 *g* rms instead of the 35 *g* previously used. A level of 70 *g* rms was used because the vibration equipment was not capable of producing higher *g* levels to simulate the expected vibration environment.

No failures were experienced when the engineering prototype sensors were evaluated at type-approval vibration levels or at 160% of type-approval levels. These sensors included a total of 14 detectors and it appeared that the resilient mount had effectively prevented vibration-induced detector failures. The proof-test-model sensors were then modified to incorporate the resilient mount in preparation for the continuation of formal type-approval testing.

The screening of the ruggedized detectors was completed in time to incorporate them into all flight sensors subsequent to the proof-test-model sensors. The uncertainty of the vibration resistance of individual non-ruggedized detectors resulted in a decision to use the ruggedized detectors for the flight sensors. This decision soon proved to be prudent because of testing experience with the proof-test sensors. As described in Section IV, two additional non-ruggedized detector failures were encountered during subsequent type-approval vibration testing. In each case the failed detector was replaced with a ruggedized detector and the testing was continued successfully.

One out-of-tolerance null condition was experienced on the first set of flight sensors during the post-environmental functional test. The null offset at 0 deg was 68 arc seconds compared to the specified tolerance of ± 54 arc seconds. It was found that a null offset can be caused by depressing the detector assembly toward one side of the resilient mount. This indicates that vibration or thermal stresses can change the null by altering the "at rest" position of the detector assembly relative to the sensor shadow edges. The tolerance of 54 arc seconds represents a shift in detector position of 0.00066 in.

The sensor assembly was reworked by lapping the mounting feet to change the mounting plane slightly relative to the shadow edges and detector position. The flight-acceptance test was re-run and the post-environmental test revealed in-tolerance conditions.

Another anomaly appeared after type-approval thermal-shock testing. The post-environmental functional tests revealed that the pitch null was 79 arc seconds compared to the specified tolerance of ± 54 arc seconds. It was decided to repeat this test with closer controls to prevent an inadvertent side force on one of the detectors, which could cause a null offset.

The thermal-shock test was repeated after the out-of-tolerance null was corrected by reworking the sensor. The post-environmental functional test revealed a pitch null offset of 107 arc seconds and a yaw offset of 112 arc seconds. These results indicate that thermal shock can induce thermal stresses that cause the detectors to come to rest at a different position within the resilient mount after testing. Sun sensors on prior missions also used resilient-mount detectors, but the configuration provided much more restraint. These sensors did not exhibit any measurable null offset due to environmental testing.

A series of seven thermal-shock tests were run to determine whether the offsets were accumulative and also to obtain more data points. The results indicated that the offsets were random in nature, sometimes changing from a plus to a minus null error in successive tests. Null offsets

from 20 arc seconds to 2.5 arc minutes were observed in the 14 data samples.

An examination was made of the feasibility of relaxing the null offset tolerance in lieu of a costly redesign and retest effort. A decision was made to change the null tolerance from ± 54 seconds of arc to ± 1.4 mrad or 4.8 minutes of arc.

In regard to the mission performance, this relaxed tolerance represents a small increase in the total target miss variance from 845 km, 1σ, to 852 km, 1σ.

B. Design and Fabrication of Sun Gate

The *Mariner* Mars 1964 sun gate design was modified for *Mariner* Mars 1969 to incorporate the same detector used in the acquisition and cruise sun sensors. Also, the mounting surface was made perpendicular to the optical axis instead of parallel to it, to allow the gate to mount on the same pedestal surface as the bay-IV cruise sensor assembly. This resulted in a simplification of the pedestal design.

The design changes allowed an improvement in the terminal board configuration. The photodetector leads were routed directly to the solder terminals of the terminal board. This eliminated four solder joints, between the terminal board and detectors, and simplified the assembly. The reduction in the number of solder joints also increased the inherent reliability. The sun gate is shown in Fig. 5b.

Initial functional tests revealed that additional baffling was needed to prevent stray light from reducing the resistance at angles greater than 5 deg. The needed baffling was accomplished by the addition of a black paint pattern on the face of the detector assembly window. This pattern provided a transparent aperture parallel to and 0.008 in. wider than the photosensitive area of the detector.

Although no failures were encountered during the environmental testing of the sun gate, the resilient mount and the ruggedized detectors were incorporated in the sun gate design to ensure against possible failures. These design modifications were made concurrently with like modifications on the acquisition and cruise sun sensors.

IV. Environmental Testing

The initial type-approval vibration test of a cruise sun sensor assembly resulted in a failure of an acquisition detector. The construction of a photodetector is illustrated in Fig. 7. An analysis of the failed detector revealed that the ceramic substrate had moved in relation to the outer parts of the assembly. This vibration-induced motion had fractured the indium solder joints connecting the electrical leads to the ceramic substrate. Movement of the substrate is normally prevented by the electrical leads, which are crimped over to hold it against the header assembly.

Lightweight accelerometers (2 g each) were mounted on a sun sensor housing assembly to monitor the approximate vibration levels at which the detectors were subjected. In tests at qualification vibration levels it was found that, at a resonant frequency of 1200 Hz, the detectors were experiencing up to 550 g rms. This occurred when the device was excited at 6 g rms. The structure also exhibited resonance at lower frequencies; however, the vibration levels were below 200 g rms.

An exploratory vibration test was run to determine the vibration levels at which the cruise sensors and sun gate would be subjected while attached to their mounting pedestals. The sensors were mounted to the pedestals, which were in turn attached to the vibration fixture. Monitoring accelerometers were used to record the vibration level near the sensor detectors.

The results of this testing showed vibration levels up to 420 g rms at a frequency of 450 Hz. Consideration was given to changing the test method on these sensors to include the use of flight-type pedestals. However, this approach was decided against, primarily because consistent results could not be assured from run to run because of changes in the test pedestals. The pedestal

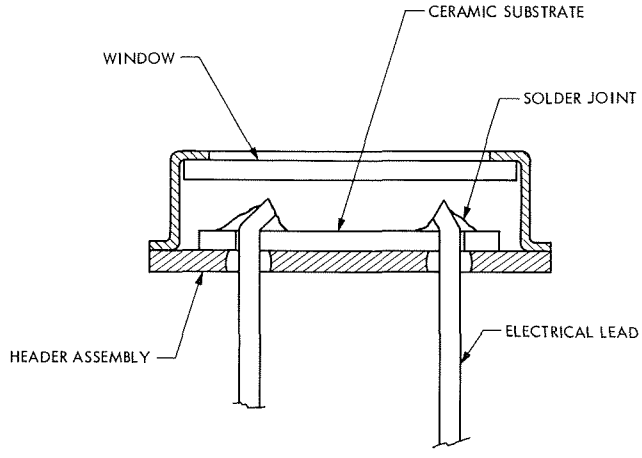

Fig. 7. Detector configuration

construction includes rivets, which were expected to loosen and thereby change the frictional damping characteristics.

The next type-approval vibration testing was done on the proof-test-model sensors after they were modified to incorporate the detector resilient mounts. Two detector failures occurred during this testing. Prior to this time it had been decided to use the ruggedized detectors for the flight sensors. In view of this, the failed detectors were replaced by ruggedized detectors and testing of the proof-test models was completed.

The first flight cruise sensors were found to be out of tolerance after flight-acceptance environmental testing. These sensors were reworked and then resubmitted for flight-acceptance testing, as described in Section III. The post-environmental tests showed these sensors to be in tolerance.

The thermal-shock test on the proof-test-model sensors also caused the null offsets to go out of tolerance. After a series of developmental thermal-shock tests, the null offset tolerance was relaxed as described in Section III. The thermal-shock test was repeated and the post-environmental testing showed the sensor nulls to be +3.78 and +2.04 minutes of arc compared to the tolerance of ±4.8 minutes of arc.

The type-approval acceleration testing of the proof-test-model sensors caused no adverse effect on their performance.

The environmental testing of the sun gate was routine, with no failures occurring.

V. Development and Fabrication of Ruggedized Photodetectors

Three design changes were made in the photodetector to increase its vibration resistance. First the header lead pins were left uncrimped. Second, the ceramic substrate of the detector was adhesively bonded to the header plate. Third, a conductive paint, in place of indium solder, was used to make the electrical connection between the detector substrate and header leads.

An evaluation of five adhesives and two conductive paints was made to determine the optimum choice as judged by the following criteria:

(1) Adequate mechanical strength throughout the expected temperature range.

(2) Sufficient chemical stability during the expected environmental conditions.

(3) Compatibility with the cadmium sulfide material. (Many adhesives contain materials that diffuse into the cadmium sulfide and permanently alter the operating characteristics.)

The test results indicated that the Eastman 910 (Tennessee Eastman Co.) would best meet the requirements for an adhesive, and Hanovia 13 (Englehard Industries) for the conductive paint. Sufficient component parts were procured from the vendor to allow construction of flight detectors. This effort was undertaken at the Jet Propulsion Laboratory in order to have flightworthy detectors available in time to support the flight hardware fabrication schedules.

A specially designed resonant-beam vibration fixture was designed and developed to amplify the g level available from the standard vibration test machine. The resonant beam is supported near each end, as shown in Fig. 8. This design allows the continuity of each detector to be monitored during testing. The central detector block can be mounted in three orthogonal positions to allow three-axis screening of detectors at 650 g rms at 850 Hz. It was decided that this test, which exceeds the expected vibration level, but only allows for one frequency, was preferable to the previous screening test, which swept from 50 to 2000 Hz, but was limited to 70 g. The natural resonant frequency of the detector substrate and header leads was calculated to be approximately 16,000 Hz, which indicates that the assembly was less sensitive to frequency than vibration level. An exploratory test on 12 non-ruggedized detectors at 650 g resulted in two failures out of 12. No vibration-induced failures resulted during the screening of 160 ruggedized detectors.

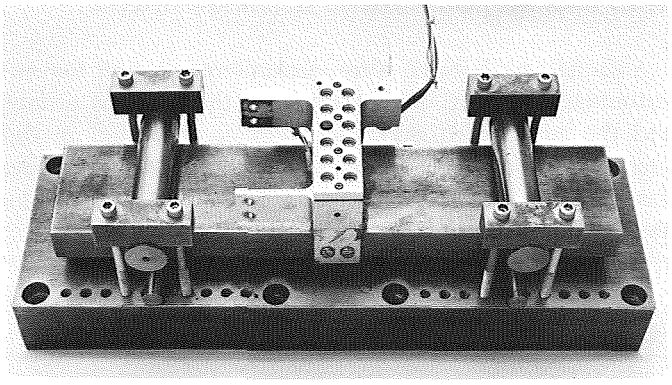

Fig. 8. Resonant-beam vibration fixture

VI. Conclusion

The development of the *Mariner* Mars 1969 sun sensors resulted in an improved, ruggedized photodetector design that was incorporated in all the flight assemblies. Among other changes made as a result of problem areas revealed during environmental testing was a resilient mount designed to reduce the high vibration levels imposed on the detector assembly. Modifications were also made in the sun gate assembly. The final flight design was verified by the successful completion of the type-approval environmental tests. The sun sensors functioned satisfactorily throughout the *Mariner* Mars 1969 mission.

For future missions, the problem of null offsets being affected by thermal shock can be avoided. The detector can be more firmly constrained, since the ruggedized version does not require a resilient mount to reduce the vibration level. For new designs it is also feasible to configure the housing so as to reduce the vibration level at the detector locations.

NASA — JPL — Coml., L.A., Calif.